Formation Kinetics of Small Gold Crystallites in Photoresponsive Polymer Gels

K. Malone,[†] S. Weaver,[‡] D. Taylor,[§] H. Cheng, K. P. Sarathy,[||] and G. Mills*

Department of Chemistry, Auburn University, Auburn, Alabama 36849

Received: January 17, 2002; In Final Form: May 8, 2002

$AuCl_4^-$ ions are transformed into Au crystallites via two consecutive photoreactions inside cross-linked polymers of diallyldimethylammonium chloride swollen with methanol. The photoreactions are markedly influenced by the gel matrix, which facilitates pathways not observed in homogeneous solutions and controls the direction of propagation. Initially, the reactions are repressed by air, but at longer times they are aided by products from the O_2-reduction. The first process is an efficient monophotonic chain reduction of $AuCl_4^-$ with chain lengths in excess of 80 and an atypical pseudofirst-order termination. Kinetic data from fully swollen gels is understood in terms of a mechanism involving solution reactions of $\cdot CH_2OH$ radical chain carriers. Light-absorbing products of the first photoreaction, believed to be gold clusters, initiate the second process that yields metal particles. Several common kinetic features are displayed by both photoreactions. However, generation of Au crystallites takes place via an unusual biphotonic chain reaction, with reaction rates that are correlated to the number of particle formation and decay cycles.

Introduction

Photoresponsive materials are interesting because their properties are reversibly altered by the presence of light. Several materials exhibiting this type of adaptive behavior have been developed, including organic and silica-based photochromic glasses,[1−4] as well as oxide films.[5] Silica photochromic glasses containing silver halide crystallites are elegant photoadaptive materials where nanometer-sized Ag particles form by the photoreduction of AgBr. Reversibility is attained via oxidation of the Ag particles in the dark that reforms the silver halide.[3] Similar reversible metal particle formation occurs by exposure of emulsions or colloids of silver halides to light pulses,[6,7] and during the evolution of Ag particles in air-saturated surfactant solutions.[8] The sensitivity of small Ag particles toward oxidation seems to be determined by size-induced enhancements in their chemical reactivity.[9,10]

Considering that small Ag and Au crystallites exhibit similar size-dependent optical properties,[11] expectations to attain a similar reversibility in the formation of gold particles under appropriate conditions appeared logical. Polymeric gels respond through reversible changes to a variety of stimuli including light.[12] However, selection of these materials as matrixes for the reversible formation of metallic gold was dictated by specific requirements of the Au chemistry, not by the photoadaptive behavior of the gels. Polymers able to swell with alcohols were considered ideal to obtain optically transparent gels, as they would permit the use of photoreactions known to yield metallic Au.[13] Swollen gels contain liquid-filled cavities, which were anticipated to restrain fast growth and aggregation of the metal crystallites. Generation of small Au particles, particularly in the diameter range of 2 to 3 nm, seemed feasible inside gels if cavity volume was related to the degree of polymer swelling. In this size range the optical properties of Au vary with particle diameter,[14] and a similar trend appeared plausible for the redox properties. Therefore, gold particles with these dimensions were expected to be thermodynamically unstable toward attack by O_2 molecules.

High Cl^- concentrations were also required in the matrix because oxidation of Au is facilitated by these ions.[15] However, growth of Au particles is accelerated by high ionic strengths.[16] Ammonium cations are known to stabilize the Au crystallites against growth,[17] and their presence in the gels was anticipated to counteract the destabilizing effect of Cl^-. Cross-linked polymers of diallyl-dimethylammonium chloride (DADMAC) swollen with methanol were found to meet all these requirements. Metal crystallites were formed upon illumination of $AuCl_4^-$ ions present inside the gels, followed by a slow particle decay in the dark.[18] Reduction of the metal complex and particle generation were distinct steps well separated in time, and both processes were faster in air-saturated gels than in the absence of air. Au crystallites with diameters larger than 2 nm formed in the gels, which, in contrast to expectations, suffered oxidation by oxygen reforming the $AuCl_4^-$ ions. A forthcoming report will be centered on the oxidation reactions. The present study examined the kinetics of the processes involved in the metal particle generation. Evidence is presented that both photoreactions proceed through free radical chain processes, with each transformation exhibiting distinct kinetic features.

Experimental Section

Methanol, formaldehyde, formic acid, H_2O_2 and HCl were obtained from Fisher. Linear poly(DADMAC) samples (average molar mass $= 2.4 \times 10^5$ g mol^{-1}) were purchased from Polysciences. $NaAuCl_4 \cdot 2H_2O$, aqueous stock solutions of DADMAC (65 wt % of monomer), CD_3OD, $CDCl_3$, and 2,4-dinitrophenylhydrazine were acquired from Aldrich. These compounds were used without additional purification. Polymers of DADMAC were prepared by γ-irradiating 20 mL of 4.16 M monomer solutions saturated with N_2 in sealed test tubes. DADMAC undergoes free radical cyclopolymerization in solutions exposed to ionizing radiation producing soluble linear

* To whom correspondence should be addressed. E-mail address: millsge@auburn.edu.

[†] Present address: IBM Microelectronics, 2070 Rte. 52, Hopewell Jct., New York 12533.

[‡] Present address: DuPont iTechnologies, Cyrel Packaging Graphics R&D, 500 Cheesequake Rd, Parlin, New Jersey 08859.

[§] Present address: Milliken, Liveoak Plant, 300 Lukken Dr., LaGrange, Georgia 30240.

[||] Present address: Department of Chemistry, Texas A&M University, College Station, Texas 77842.

10.1021/jp020176i CCC: $22.00
Published on Web 07/09/2002

polymers containing five-membered cyclic structures.[19] Exposure of the solutions to radiation doses of $0.9-1.3 \times 10^2$ kGy (dose rate = 1−1.4 kGy h^{-1}) caused cross-linking and entanglement of the cationic macromolecules yielding insoluble, solid transparent polymer cylinders, which were swollen by CH_3OH or H_2O forming polymeric gels. ^1H NMR analysis confirmed the identity of the gels since their signals matched those of cross-linked D_2O-swollen poly(DADMAC) made from linear polymers using the monomer as a cross-linking agent.[19] Signals from olefinic protons of DADMAC were not detected; comparisons with blanks indicated that less than 1×10^{-2} M of unpolymerized monomer was present in the gels.

Stock solutions with [DADMAC] = 3.85 M were used in our previous study, and the resulting gels exhibited shorter induction periods prior to metal particle formation.[18] Radiolysis of solutions containing 4.16 M monomer produced sturdier polymers that aged slower; only gels made from these polymers were employed in the present investigation. The DADMAC polymers were aged at room-temperature inside the sealed tubes for 2−4 days to complete any post-irradiation cross-linking. Longer aging times increased polymer rigidity; such undesirable change was prevented by storing the polymers at −80 °C. Swelling of the poly(DADMAC) cylinders occurred preferentially in the radial direction. Thus, cylindrical samples (1 cm long, 0.5 cm in diameter, mass = 0.16−0.18 g) were cut perpendicular to the main axis of the solid polymers, and placed vertically inside modified optical tubes. This method ensured that swelling took place mainly along the vertical axis of the samples. No changes in the photoreactions were noticed using samples cut parallel to the main axis of the polymers.

Gels were prepared by swelling the polymer samples with solutions of $NaAuCl_4$ in methanol; unless otherwise stated the $AuCl_4^-$ concentration was 1×10^{-2} M and the ratio of polymer mass to solution volume (PM/SV) was 3.8×10^{-2} g mL^{-1}. Swelling was carried out in tightly closed optical tubes to avoid solvent evaporation, and lasted 3 days at room temperature and in the dark; longer swelling periods had no effect on the kinetic data. Only gels free of voids were employed; blank experiments using polymers swollen with pure methanol showed that light absorption by poly(DADMAC) is negligible at $\lambda > 220$ nm. A small volume of solution remained on top of the gels after swelling, formation of particles in the solutions was suppressed by shielding this section from light. Gels saturated with gases other than air were prepared inside a glovebag filled with the desired atmosphere. Solutions of $NaAuCl_4$ in methanol were bubbled with a particular gas for 20 min and placed in the glovebag overnight along with the polymer samples. After the swelling period of 3 days, the optical tubes were sealed with an epoxy resin (Varian) to avoid air leaks. Water from a Millipore Milli-Q-Plus system was used in all cleaning procedures; glassware that came in contact with gold solutions was treated with aqua regia.

Air-saturated gels containing 10 mM $AuCl_4^-$ made from different batches of the solid polymer and photolyzed at constant light intensity (I_0) exhibited induction periods that varied between 75 and 150 min, whereas the rates of particle formation ranged from 4 to 19 $\times 10^{-6}$ M min^{-1}. Variations in the properties of gels are not unusual since accurate control of cross-link densities during polymerization is not feasible.[21] Very slow photoreactions occurred when stiff and highly cross-linked polymers were employed, which supports this interpretation. Less pronounced deviations (40%) were noticed for series of gels made from the same solid poly(DADMAC) cylinder. Thus, a method employing a standard gel was adopted, in which the first sample from a certain DADMAC solid polymer was always swollen with a 1×10^{-2} M $AuCl_4^-$ solution. Reaction rates of this standard were measured using $I_0 = 3.2 \times 10^{-6}$ M($h\nu$) min^{-1} and were compared with those of subsequent gels made from the same poly(DADMAC) solid. Unless otherwise stated all kinetic results were obtained during the first cycle of particle formation and decay.

Square optical cells were not affected when gels were prepared inside them, but invariably shattered after Au particles were photogenerated. Thus, the poly(DADMAC) samples were swollen inside Milton Roy #33−17−80 optical test tubes (path length (l) = 1 cm, cutoff at $\lambda \leq 300$ nm) that were flattened on the bottom. Quartz tubes having the same dimensions as the Milton Roy tubes were employed on a few occasions. Glass tubes (8 cm long, 1 cm diameter) were fused to the tops of the optical tubes. The glass tubes had #9 Chem threads on their open ends, and were closed by screwing them to sealed capillaries terminated with a combination of #7 Ace electrode/Teflon septum/nylon bushing. These alterations resulted in modified optical tubes with an internal volume of 14.5 mL, and allowed experiments to be conducted for more than 4 months without significant losses of CH_3OH. Uniform illumination of the gels was ensured by positioning the optical tubes vertically in the center of a Rayonet 100 circular illuminator, where the temperature was 29 °C. Photons with $\lambda = 350 \pm 15$ nm were used, which were generated from RPR-3500A lamps. Light intensity determinations were performed for every kinetic run employing the Aberchrome 540 actinometer.[20] Except for illuminations with variable light intensities, I_0 was maintained at 3.2×10^{-6} M($h\nu$) min^{-1}. Calculation of quantum yields requires an evaluation of the fraction of photons absorbed by the chromophores, but accurate estimates of this number are difficult to obtain due to changes in [chromophore], and because the produced Au particles absorb at 350 nm. Thus, photonic efficiency (PE) values were used in this study, which correspond to the reaction rate divided by the light intensity measured by the actinometer. These values can be considered as lower limits of the quantum yields.

UV−vis spectra of the gels were recorded at room temperature with a Hitachi U-2000 spectrophotometer or a Hewlett-Packard 8452 diode array instrument. The center of the analyzing beam entered the samples at about 0.9 cm from the bottom of the optical tubes in the Hitachi instrument. Because the analyzing light extended only 0.3 cm below the beam center, raising the tubes by 5 mm from their normal position in the sample holder permitted monitoring the early stages of the photoreactions. An analogous arrangement was used for measurements with the diode array spectrophotometer. Attempts to quantify $[H_2O_2]$ in the gels by means of iodometric methods failed because of interfering reactions between I^- and $AuCl_4^-$. Methanol extracted from irradiated gels with $CDCl_3$ was analyzed by means of FTIR as well as by ^{13}C and ^1H NMR techniques with TMS as a reference standard. 2,4-Dinitrophenylhydrazine was used for the detection of CH_2O in CH_3OH. FTIR and NMR measurements were done on a Bruker Equinox 55 and a Bruker AC 250 spectrometers, respectively. Collection of powder X-ray diffraction (XRD) data was carried by means of a Siemens D5000 diffractometer using Cu K_α radiation.

Au colloids were prepared under conditions simulating as close as possible the gel environment. Mixtures of 70% CH_3OH and 30% H_2O (v/v) allowed solubilization of 2.8×10^{-5} M linear poly(DADMAC) that acted as a particle stabilizer. Exposure of air-saturated mixtures containing 5×10^{-5} M $AuCl_4^-$ to 350 nm photons for 96 min yielded stable red

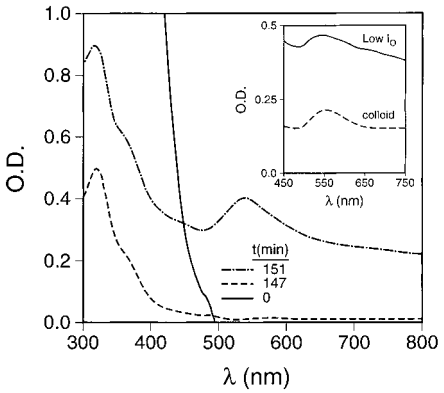

Figure 1. Evolution of the optical spectra with time for an air-saturated poly(DADMAC) gel containing 1×10^{-2} M $AuCl_4^-$ irradiated with $I_0 = 3.2 \times 10^{-6}$ M($h\nu$) min^{-1}. Inset: (top) spectrum of Au particles made in a gel with $I_0 = 7.9 \times 10^{-7}$ M($h\nu$) min^{-1}; (bottom) spectrum of a colloid made in a 70% CH_3OH/30% H_2O solution with 5×10^{-5} M $AuCl_4^-$, 8×10^{-5} M linear poly(DADMAC) and $I_0 = 3.1 \times 10^{-6}$ M($h\nu$) min^{-1}.

colloids. The spectrum of the colloids exhibited the characteristic surface plasmon of Au particles with a maximum at 525−530 nm (Figure 1, inset). An extinction coefficient (ϵ) of 2.6×10^3 M^{-1} cm^{-1} (per mole of Au atoms) at 525 nm was obtained using optical density (O.D.) values from serial dilutions of the colloids, which is in good agreement with prior determinations.[22] Transmission electron microscopy measurements carried out on a Zeiss EM 10CR microscope yielded an average diameter of 11 nm for the spherical Au particles.

Results

Poly(DADMAC) samples swollen with $AuCl_4^-$ solutions produced yellow gels as a result of the ligand-to-metal charge transfer (LMCT) band of this complex above 300 nm.[13] The strength of the metal ion absorptions was determined in CH_3OH solutions of $AuCl_4^-$ containing 1 M DADMAC to attain an environment close to that of polymers swollen with at PM/SV $= 3.8 \times 10^{-2}$ g mL^{-1}, including the same [Cl^-] (estimated to be 1 M in these gels, without considering the polymer volume). In these solutions $\epsilon = 3.4 \times 10^4$ M^{-1} cm^{-1} for the high energy CT band centered at 228 nm, $\epsilon = 5.93 \times 10^3$ M^{-1} cm^{-1} for the absorption with $\lambda_{max} = 320$ nm whereas $\epsilon = 144$ M^{-1} cm^{-1} at 360 nm. These values agree well with earlier determinations in 2-propanol.[13] As illustrated in Figure 1, spectra of gels with 1×10^{-2} M $NaAuCl_4$ exhibited a tail extending beyond 400 nm since the signal centered at 320 nm was very strong and broad at this high [$AuCl_4^-$].

Illuminations of the gels bleached the absorption of $AuCl_4^-$ because the metal ion is photoreduced to $AuCl_2^-$ in alcohols ($\lambda_{max} = 246$ nm, $\epsilon = 212$ M^{-1} cm^{-1}).[23] Photolysis in quartz tubes yielded a weak shoulder at about 247 nm (O.D. < 0.5) next to the high energy LMCT band of $AuCl_4^-$. Hence, the bleaching process generated less than 2 mM Au(I). The bleaching step, or induction period, took place prior to metal formation; during this period the gels turned progressively colorless inward from the polymer-glass interface, proceeding from bottom to top of the samples. Included in Figure 1 is a spectrum recorded at the end of this period (147 min) exhibiting a shoulder centered at about 360 nm that persisted throughout the photolysis. The residual optical density at 320 nm is evidence that some $AuCl_4^-$ ions were present after the induction period. This signal decayed slowly upon further illumination, which also resulted in broad absorptions above 500 nm together with continuous shifts of

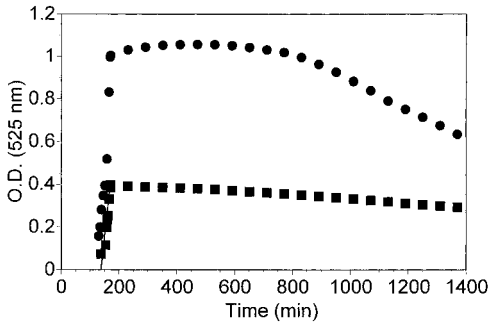

Figure 2. Temporal evolution of the gel absorbance at 525 nm, illumination was stopped once the O.D. of the Au particles reached 0.3 (■) and 1.22 (●). The straight line connecting the squares corresponds to the fit O.D. $= 1.2 \times 10^{-2}$ $t - 1.2$ ($r^2 = 0.992$).

λ_{max} from 520 to 530 nm. Figure 1 shows a spectrum collected after 151 min displaying the typical surface plasmon of Au crystallites at $\lambda > 500$ nm.[11] The higher intensities of the signals at 360 and 320 nm are obviously a consequence of the strong absorption below 400 nm of the metal particles.

Illustrated in Figure 2 is the evolution of the particle absorption at 525 nm as a function of time. In the lower curve photolysis was discontinued once an absorbance of 0.3 was reached, whereas light-exposure was terminated upon achieving an absorbance of 1.22 in the top curve. Linear increases of O.D. followed in both cases after an induction period of about 110 min, which are consistent with the apparent zero-order kinetics of particle formation that was demonstrated in our previous study.[18] Additional particles were produced via a persistent post-irradiation step especially when the absorbance was close to 1; this process was less pronounced and shorter when lower optical densities were attained. Although no such step occurred at the end of the induction period, an analogous post-irradiation growth of the absorbance occurred when the photosynthesis of Au colloids (as described above) was not run to completion. In gels, the optical density at 525 nm decreased at longer times as the metal particles were oxidized, but for O.D. ≤ 0.5 the combined processes of particle oxidation and total regeneration of $AuCl_4^-$ lasted 15 days. Longer times were needed for complete reformation of the metal ions when O.D. increased above 0.5 during photolysis. Hence, illumination was stopped in most cases once the absorbance at 525 nm reached between 0.3 and 0.5 to avoid very long kinetic runs.

The peculiar chemistry observed in the gels mandated independent confirmation that metallic particles were responsible for the absorption changes displayed in Figure 2. XRD measurements provided evidence that Au crystallites were generated during photolysis, the results are presented in Figure 3. Reflections from the {111} and {200} lattice planes of fcc Au were observed at 2Θ angles of 38.3° and 44.4°, which were absent in the diffraction pattern of poly(DADMAC) shown in the inset. These results were obtained from powder samples made by drying the gels under vacuum (to stop any particle decay) followed by grinding. Analysis of the signal line width with the Scherrer equation yielded an average particle diameter of 35 nm. Such large sizes are probably a product of the long photolysis periods (8 h) needed for generation of enough crystallites to allow their detection by XRD. Metal formation started in regions of the gel closest to the tube wall, continuing inward and from bottom to top. As was shown in our earlier study,[18] alternating irregular layers of orange and red particles were generated in gels made with 3.85 M solutions of monomer. Random domains of colored particles prevailed in gels prepared from 4.16 M DADMAC solutions; patterned structures with

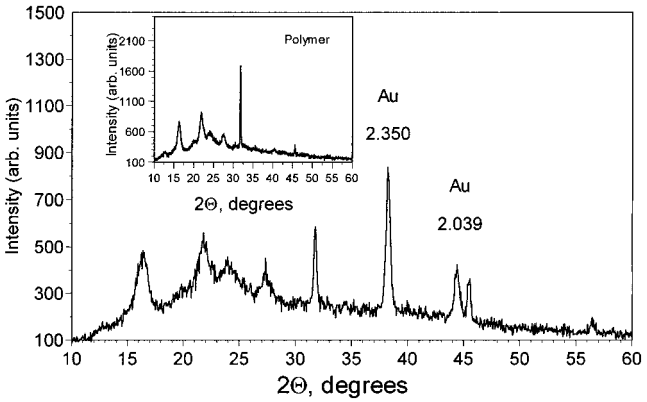

Figure 3. XRD powder pattern of a dry gel containing 1×10^{-2} M $AuCl_4^-$ photolyzed for 8 h. Inset: diffraction pattern of cross-linked solid poly(DADMAC).

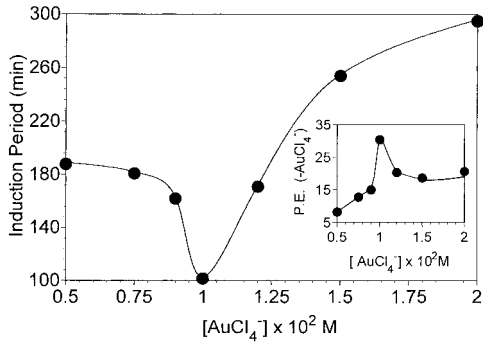

Figure 4. Changes in the induction period as a function of $[AuCl_4^-]$ for gels illuminated with $I_0 = 3.2 \times 10^{-6}$ M($h\nu$) min^{-1}. Inset: photonic efficiencies of $AuCl_4^-$ photobleaching vs metal ion concentration.

regular layers spaced at 0.8 mm were noticed occasionally. Despite these differences, the crystallite generation rates were very similar in all systems; the first particles produced were always orange but turned red with further illumination. Further experiments with gels having their lower section shielded from light yielded Au particles only in the mid-section exposed to photons, and no crystallite migration occurred. These results demonstrate conclusively that metal formation starts on the bottom of unshielded gels, and exclude a possible precipitation of particles formed in the upper sections of the swollen polymers.

The effect of $[AuCl_4^-]$ on the photoreactions was studied in gels made from solutions containing 5×10^{-3} M to 2×10^{-2} M of the metal ion. At $[AuCl_4^-] < 5$ mM only the bleaching step occurred, whereas the upper concentration limit was imposed by the solubility of the gold complex in CH_3OH. Shown in Figure 4 is the effect of $AuCl_4^-$ concentration on the induction period. This period shortened from 190 to 170 min when $[AuCl_4^-]$ changed from 5 to 9.5 mM, reaching a minimum of 100 min at 1×10^{-2} M, and increased significantly at higher concentrations. Irrespective of experimental conditions ($[AuCl_4^-]$, I_0, or PM/SV) the end of all induction periods was characterized by O.D. values at 320 and 360 nm of 0.5 and 0.2, respectively. However, the remaining $AuCl_4^-$ ions were confined to regions that appeared as vertical cylinders having central axes coinciding with the center of the gels. Zones beyond these regions and closer to the tube wall were free of Au(III) ions. The cylinder diameters were only a function of Au(III) concentration and increased from 0.2 to 0.5 cm and to 0.7 cm when $[AuCl_4^-]$ was raised from 5 mM to 10 mM and then to 20 mM. Using Beer's law these diameters were employed first to estimated the $[AuCl_4^-]$ within the cylinders, followed by calculation of the absorbance at 360 nm due to the Au(III) ion. This O.D. was 1.2×10^{-2} in all cases, meaning that the induction period ended when the species with an optical signal centered at 360 nm had an absorption at this wavelength (0.188) 16 times stronger than that of the remaining $AuCl_4^-$.

In view of the low concentration of Au(III) left unreduced ($\leq$ 4% of the initial amount), calculations of rates were simplified assuming that these ions were uniformly distributed within the gels. This approximation together with the O.D. at 320 nm yield a $[AuCl_4^-]$ persisting at the end of all induction periods of 8.4×10^{-5} M (using $l = 1$ cm). Rates of photoreduction, $r(-AuCl_4^-)$, were evaluated from the $[AuCl_4^-]$ change divided by the length of the induction period. Photonic efficiencies for the reduction, $PE(-AuCl_4^-)$, were calculated from the reduction rates and are shown in the inset of Figure 4. The efficiencies increased linearly from 8 to 15 between 5 and 9.5 mM Au(III), according to: $PE(-AuCl_4^-) = 1.7 \times 10^3 [AuCl_4^-] - 7.2 \times 10^{-2}$ ($r^2 = 0.997$). $PE(-AuCl_4^-)$ reached a maximum of 32 at 10 mM Au(III) and decreased to around 22 at higher concentrations.

Attempts to obtain $r(-AuCl_4^-)$ values directly from the decrease in O.D. at 320 nm as a function of time in gels containing 1×10^{-2} M $AuCl_4^-$ were unsuccessful because the absorbance remained above 2 through most of the induction period; a reproducible collection of data in the final stages of this period was impossible because of abrupt and fast changes of optical density. The drastic absorption changes also hampered efforts to investigate the formation kinetics of the species with an absorption centered at 360 nm. Determination of $r(-AuCl_4^-)$ from the decay rates of O.D. at $\lambda \geq 400$ nm was also attempted, a method valid solely for the early reduction stages when $[AuCl_4^-]$ is high because this region $\epsilon < 100$ M^{-1} cm^{-1}. The changes in absorbance were very small, indicating that processes other than the reduction of $AuCl_4^-$ predominated during this time. This interpretation was validated by an experiment where a gel with 1×10^{-2} M $AuCl_4^-$ was photolyzed for 80 min, reaching an O.D. of 1.5 at 320 nm. The gel was placed overnight at 4 °C to avoid any dark reaction, and then heated to room temperature followed by illumination. Another induction period of about 80 min was noticed before further bleaching continued. Because any oxygen reduced by the first illumination was replenished during the dark term, the findings mean that O_2 inhibited the photoreduction of $AuCl_4^-$. Obviously, oxygen consumption was dominant through most of the induction period; fast reduction of the metal complex occurred mainly at the end of this period when $[O_2]$ was low. Thus, $r(-AuCl_4^-)$ was underestimated in calculations that employed the full length of this induction period, implying that the values of P. E.$(-AuCl_4^-)$ are lower limits of the photonic efficiencies of metal ion reduction.

Illumination past the induction period resulted in a linear increase with time of the optical signals due to metal particles in all experiments. Rates of O.D. increase at 525 nm were calculated using the slopes of the straight lines generated from zero-order plots similar to those of Figure 2. As was shown earlier,[18] Au crystallites were formed within circular gel zones next to the tube wall and outside the cylindrical regions still containing unreduced $AuCl_4^-$, where a very slow reduction of Au(III) took place. Thus, a corrected path length was employed in the calculation of the rates of O.D. increase that excluded the diameter of the cylindrical regions. Au crystallites made in the gels have optical spectra that resemble the spectra of colloids prepared as described above (see inset of Figure 1). Therefore, the rate of particle formation in gels, $r(Au_n)$, was computed using the ϵ value of colloidal gold at 525 nm. The rates are presented

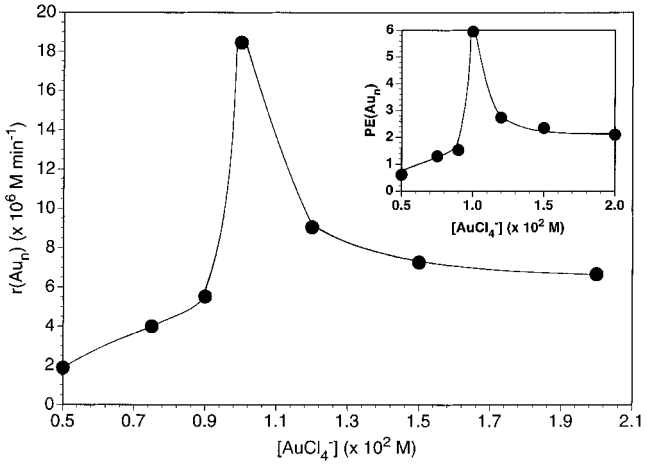

Figure 5. Dependence of the metal particle formation rate on [$AuCl_4^-$] for gels irradiated with $I_0 = 3.2 \times 10^{-6}$ M($h\nu$) min^{-1}. Inset: photonic efficiencies of Au particle formation as a function of $AuCl_4^-$ concentration.

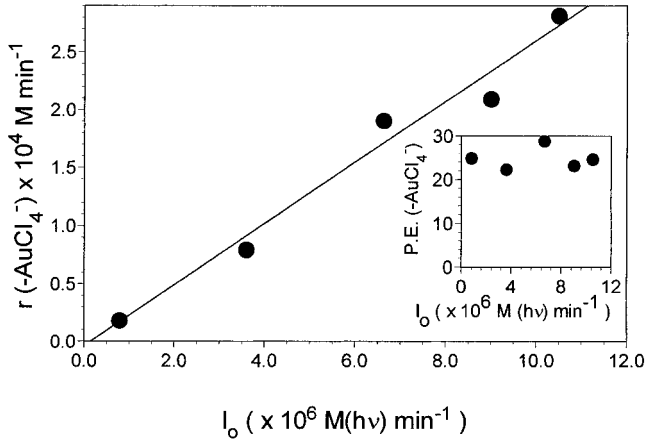

Figure 6. Variations in $r(-AuCl_4^-)$ with I_0 for gels containing 1×10^{-2} M $AuCl_4^-$. The inset demonstrates the independence of PE($-AuCl_4^-$) on light intensity.

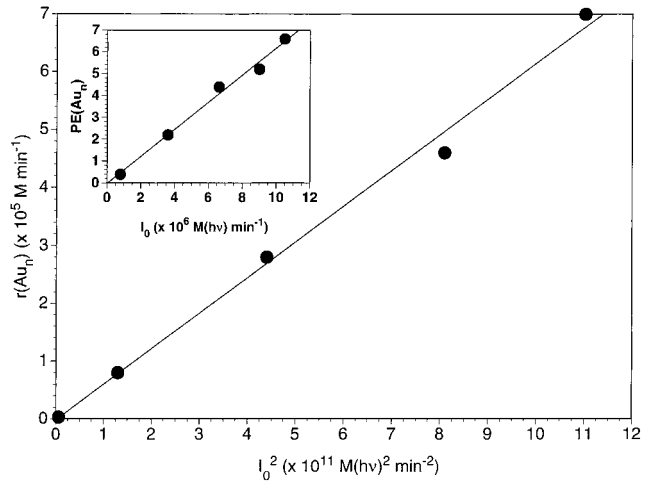

Figure 7. Dependence of $r(Au_n)$ on $(I_0)^2$ for gels with 1×10^{-2} M $AuCl_4^-$. The inset shows that PE(Au_n) is a linear function of light intensity.

in Figure 5 and show that $r(Au_n)$ increased slightly in the range $5 \leq [AuCl_4^-] \leq 9$ mM, then abruptly to a maximum of 1.9×10^{-5} M min^{-1} at 10 mM Au(III) followed by a large decrease at higher concentrations.

Values of the photonic efficiency of particle formation, PE(Au_n), are included in the inset of this Figure. PE(Au_n) increased gradually from 0.6 to 1.3 when [$AuCl_4^-$] varied from 5 to 9 mM, followed by a maximum efficiency of 6 at 1×10^{-2} M. Thereafter, PE(Au_n) decreased to a value of 2.1 at the highest concentration of metal ions. Worth noting is that the procedure for determining $r(Au_n)$ underestimates the true rate of particle formation because: (a) corrections for the multiphotonic nature of this process (see below) were not possible, (b) absorption of photons at 350 nm by existing crystallites was not accounted for, and (c) the cogenerated smaller (orange) Au particles exhibit a weaker plasmon than larger (red) metal crystallites, see inset of Figure 1.[14] Hence, the reported PE(Au_n) are lower limits of the photonic efficiencies of metal particle generation.

Altering the metal ion concentrations in the methanolic solutions had no visible effect on the extent of polymer swelling at [$AuCl_4^-$] $\leq 1 \times 10^{-2}$ M, where the gel height remained constant at 4.5 cm. Swelling along the vertical axis decreased continuously at higher concentrations, reaching a height of only 3.5 cm at 2×10^{-2} M Au(III). Introduction of 1M DADMAC monomer (or HCl) into 1×10^{-2} M $AuCl_4^-$ solutions reduced swelling slightly (15%). Although the length of the induction period remained unchanged, $r(Au_n)$ was 1.8 times lower than for gels free of these electrolytes. In contrast, polymer swelling was not altered by the presence of 1 M CH_2O or HCO_2H (which is not ionized in CH_3OH), and neither were the induction period or $r(Au_n)$. Further swelling studies employed a constant polymer mass but the volume of the $AuCl_4^-$ methanolic solution was varied by factors of 0.75, 1.5 and 2, yielding PM/SV ratios of 5.04×10^{-2}, 2.5×10^{-2}, and 1.9×10^{-2} g mL^{-1}, respectively. Although the larger volumes of solution enhanced polymer expansion, the induction periods and $r(Au_n)$ values remained constant for gels having a PM/SV ratio $\leq 3.8 \times 10^{-2}$ g mL^{-1}. However, gels made with the lower volume of $AuCl_4^-$ solution (PM/SV $= 5.04 \times 10^{-2}$ g mL^{-1}) exhibited not only less pronounced swelling (2.5 cm of gel height), but the induction periods were twice as long and $r(Au_n)$ declined by a factor of 54.

Changes in the intensity of light affected considerably the photoreactions in the gels since increases in I_0 from 7.9×10^{-7} to 1.1×10^{-5} M($h\nu$) min^{-1} shortened the induction periods from 500 to 38 min. Figure 6 demonstrates that the corresponding $r(-AuCl_4^-)$ values changed linearly (slope $= 26.4$) with increasing I_0. Thus, as shown in the inset, a constant PE($-AuCl_4^-$) average value of 26 was obtained at all light intensities. The rates of particle generation were very sensitive to light intensity; the data of Figure 7 indicates that $r(Au_n)$ changed linearly with $(I_0)^2$. As expected for a biphotonic reaction, the resulting PE(Au_n) values presented in the inset were a linear function of light intensity. Larger (red) crystallites displaying the characteristic surface plasmon predominated in all cases except at the lowest photon flux, where the gel turned orange and exhibited broad and weak signals above 500 nm analogous to the top spectrum of the inset in Figure 1. Orange gels with similar spectra resulted at $I_0 = 3.2 \times 10^{-6}$ M($h\nu$) min^{-1} only under conditions that retarded particle formation, such as in polymers swollen with solutions containing 1 M HCl.

Earlier findings hinted that the rates of the photoreactions were affected by the number of particle formation and decay cycles.[18] The present data show that the induction period shortened and that particles formed faster with growing number of cycles. Photonic efficiencies for the $AuCl_4^-$ reduction step are presented in Figure 8, included in the inset are the PE(Au_n) values. Two series of experiments were performed using intervals between successive cycles of either 3 or 14 days. Because 15 days are needed to attain the initial [$AuCl_4^-$], reformation of the Au(III) complex was more extensive for the

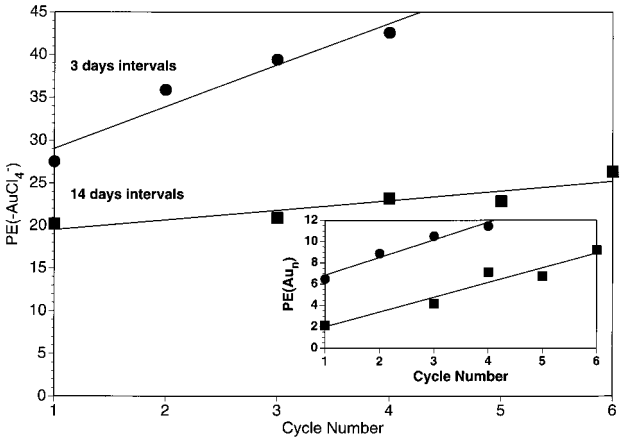

Figure 8. Changes in PE($-AuCl_4^-$) with number of particle formation and decay cycles for gels stored (●) 3 days and (■) 14 days in the dark between cycles, $[AuCl_4^-] = 1 \times 10^{-2}$ M and $I_0 = 3.2 \times 10^{-6}$ M($h\nu$) min^{-1}. Inset: Variations in PE(Au_n) with number of cycles; the symbols indicating the length of the dark period are the same as for the main figure.

series with the longer dark period. PE($-AuCl_4^-$) increased in a more pronounced fashion when the interval between cycles was shorter. On the other hand, large but similar increases of PE(Au_n) were detected irrespective of the interval length. In fact, this "memory effect" was lost only after leaving the exposed gels for several months in the dark.

Evidence of the strong influence by the gel matrix on the photoreactions of $AuCl_4^-$ was obtained during the synthesis of the Au colloid described above. Illumination of solutions containing 5×10^{-5} M metal ions and linear poly(DADMAC) yielded PE($-AuCl_4^-$) = 3.2 and PE(Au_n) = 0.4, whereas no Au particles were formed in gels with [Au(III)] < 5×10^{-3} M. For this reason, attempts were made to determine whether components of the gel system influenced the photoreactions. The light-induced optical changes in the gels were similar to those accompanying the dark generation of colloids at room temperature when OH^- ions are added to solutions of $AuCl_4^-$ in CH_3OH.[24] Unlike these systems, where the reaction is accelerated by silica surfaces, photoreaction speeds remained unchanged when the optical tubes consisted of either quartz or borosilicate glass. $AuCl_4^-$ was not reduced in the absence of light even after maintaining the gels at 40 °C for several hours. Thus, the photoreactions were neither catalyzed by SiO_2, nor a consequence of dark transformations accelerated by heating effects of light, as reported for some photochromic systems.[12]

The rates of the photoreactions remained unchanged upon substitution of CH_3OH by CD_3OD. Large decreases in both PE($-AuCl_4^-$) and PE(Au_n) occurred when [CH_3OH] in the swelling solutions were systematically lowered by addition of H_2O. Gels with pH 6.3 were made upon swelling poly(DADMAC) with aqueous solutions of 10 mM $AuCl_4^-$. The complex was reduced under similar conditions in water by several polymers to Au particles.[25] No such reactions took place in aqueous gels after extensive illumination, excluding a possible reduction of $AuCl_4^-$ by the polymer. Carbonyl signals were detected in both FTIR and ^{13}C NMR measurements of CH_3OH extracted from gels after particles were formed. Reaction of the extract with 2,4-dinitrophenylhydrazine confirmed that CH_2O was produced by photolysis. Formaldehyde was not detected in unirradiated gels.

Experiments using gels saturated with either 50/50 mixtures of N_2/O_2 or with pure O_2 corroborated that oxygen competed with the Au(III) photoreduction. The induction periods increased by 1.6 and 3.6 times respectively; whereas PE(Au_n) was the same in gels with the N_2/O_2 mixture or with air, particle formation was 12 times less efficient in gels with 1 atm O_2. As mentioned above, a slow regeneration of $AuCl_4^-$ took place instead of post-irradiation formation of particles when illumination was stopped at the end of the induction period. Au crystallites were produced immediately if photolysis was interrupted for up to 15 min; for longer dark intervals, particles formed only after an induction time proportional to the length of the period without light. Long illumination times were also needed to restart crystallite formation when the dark particle-oxidation process was allowed to occur for several hours. Because part of the O_2 consumed by photolysis was replenished during the dark periods, these findings indicate that high oxygen concentrations in the gels restrain crystallite generation.

Interestingly, in N_2-saturated gels, the induction period increased by at least 70%, PE(Au_n) was 5 times smaller, and no post-irradiation formation of Au crystallites occurred. Opening the sealed N_2-containing gels to air after total reformation of $AuCl_4^-$ and exposing them again to light yielded the higher reaction rates typical of air-saturated gels, confirming the efficiency decreases in the presence of N_2. Thus, although the $AuCl_4^-$ photoreduction and crystallite formation are retarded by O_2, these reactions are more efficient in systems prepared with air. No changes in $r(-AuCl_4^-)$ or $r(Au_n)$ were detected when H_2O_2, the expected product of the O_2 reduction, was added to air-saturated gels at concentrations in the mM range or lower. In contrast, the presence of 1×10^{-2} M H_2O_2 altered the induction period and $r(Au_n)$ in a way comparable to the changes noticed for oxygen-saturated gels ($[O_2] = 8.2 \times 10^{-3}$ M in CH_3OH).[26]

Discussion

The findings of the present study indicate that the photoreduction of $AuCl_4^-$ ions inside the gels shares some kinetic features with homogeneous photoreactions in alcohols including methanol. $AuCl_4^-$ is photobleached in alcohols which act as reducing agents;[13] $AuCl_2^-$ ions have been detected as a product in ethanol.[23] However, no chain reduction of Au(III) occurs in these systems or during radiolysis of degassed aqueous solutions in the presence of 2-propanol.[22] Furthermore, the efficiency of the Au(III) photoreduction in alcohols is not altered by variations in $[AuCl_4^-]$ or I_0.[13] In contrast, the PE($-AuCl_4^-$) values of Figures 4, 6, and 8 are evidence that the metal ions are photobleached in the gels via a chain reaction that depends on I_0 and $[AuCl_4^-]$. The chain reduction occurs as well in homogeneous solutions of linear poly(DADMAC) even at low $[AuCl_4^-]$, highlighting the significant role that the polymer plays in the photoreactions.

CH_3OH participates in the photobleaching process because the reaction efficiency is decreases when the [alcohol] is lowered by addition of H_2O. EPR measurements showed that alcohol radicals form by photolysis of $AuCl_4^-$ in solution,[13] and the inhibiting effect of O_2 indicates that the radicals are involved in the Au(III) reduction. Photobleaching is more efficient in gels that initially contain air, suggesting that the reduction of Au(III) is aided by a product of the O_2-consumption step. A photonic efficiency of 6.6 results, assuming that the latter reaction requires 80 min (a conservative estimate) for completion in air-saturated CH_3OH ($[O_2] = 1.7 \times 10^{-3}$ M).[26] Evidently, oxygen is also reduced via a chain process, $AuCl_4^-$ is the only species able to absorb the 350 nm photons and is, therefore, the most logical sensitizer for this transformation. Although

elucidation of the reaction mechanism is beyond the scope of the present study, peroxyl radicals derived from CH_3OH are obvious intermediates.[27] The Au(III)-sensitized photoreduction of O_2 may be represented by the overall reaction

$$CH_3OH + O_2 + h\nu \rightarrow H_2O_2 + CH_2O \quad (1)$$

It should be noted that hydroxymethylhydroperoxide (HO_2CH_2OH) is not only one of the expected products of this reaction in CH_3OH, but also exists in equilibrium with H_2O_2 and CH_2O.[28] For simplicity, H_2O_2 was presumed to be the product of the O_2-reduction that aids the photobleaching of Au(III). Direct reduction of $AuCl_4^-$ by H_2O_2 is inhibited by $[Cl^-] \geq 0.1$ M,[29] and no such reaction was detected after introducing peroxide into the gels. Changes in the photobleaching kinetics were not observed in gels prepared using solutions with $[H_2O_2] \leq 1$ mM, which is not surprising considering that peroxide disproportionation (to yield O_2 and H_2O) in the presence of Au(III) is likely during the long times needed for complete swelling of the polymers. Although inconclusive results were obtained in these experiments, H_2O_2 is known to accelerate the $AuCl_4^-$ photoreduction in homogeneous solution.[30] Therefore, participation of a peroxide in this photoreaction still seems the most reasonable explanation for some of the kinetic effects detected in gels with air.

Reduction of $AuCl_4^-$ turns significant once most of the O_2 is consumed, at which point the radicals of CH_3OH react predominantly with the metal complex. Formation of the radicals by excitation of $AuCl_4^-$ with 350 nm light is believed to involve electron transfer from a coordinated Cl^- to the metal center due to the LMCT nature of the absorption bands, generating $\cdot Cl$ and Au(II).[13,31] Cl atoms react fast with methanol by hydrogen-abstraction to form $\cdot CH_2OH$ radicals and HCl. Slow ligand exchange of one Cl^- by CH_3OH occurs in this solvent,[29] allowing another formation path for $\cdot CH_2OH$ that involves oxidation of a methanol molecule coordinated to the excited Au center. However, the high $[Cl^-]$ in the gels lowers the probability of such substitution process. Nevertheless, an overall step (reaction 2) able to represent both pathways is used to describe the generation of $\cdot CH_2OH$ in the mechanism. The following sequence of steps can account for most of the results shown in Figures 4 and 6 and for the formation of CH_2O as principal organic byproduct

$$AuCl_4^- + CH_3OH + h\nu \rightarrow AuCl_4^{2-} + \cdot CH_2OH + H^+ \quad (2)$$

$$AuCl_4^- + \cdot CH_2OH \rightarrow AuCl_4^{2-} + CH_2O + H^+ \quad (3)$$

$$AuCl_4^{2-} + CH_3OH \rightarrow AuCl_2^- + \cdot CH_2OH + 2Cl^- + H^+ \quad (4)$$

$$\cdot CH_2OH + H_2O_2 \rightarrow \cdot OH + H_2O + CH_2O \quad (5)$$

$$\cdot OH + CH_3OH \rightarrow \cdot CH_2OH + H_2O \quad (6)$$

$$\cdot CH_2OH + H_2O_2 \rightarrow HO_2\cdot + CH_3OH \quad (7)$$

$$\cdot CH_2OH + HO_2\cdot \rightarrow CH_2O + H_2O_2 \quad (8)$$

Step 4 is a composite propagation reaction in which a $\cdot CH_2OH$ radical is generated through reduction of the Au(II) complex by the solvent. Such process seems reasonable in view of the very fast ligand exchange by Au(II),[32] facilitating coordination of CH_3OH to the metal center and then oxidation of this molecule. In water, ligand exchange competes with the fast disproportionation of $AuCl_4^{2-}$ to $AuCl_2^-$ and $AuCl_4^-$, $k = 4.8 \times 10^8$ M^{-1} s^{-1}.[33] Chain termination via Au(II) disproportionation is not expected to compete effectively with the exchange of Cl^- by CH_3OH in the gels due to their very high [methanol] (>20 M). Also, lower disproportionation rates of $AuCl_4^{2-}$ are anticipated in our polyelectrolyte gels since strong electrostatic attractions between the cationic polymer backbone and counterions occur in these systems. For instance, the diffusion coefficient of trivalent counterions can decrease by 2×10^3 times in poly(DADMAC) gels as compared with the solution value.[34] Attractions between the cationic groups of poly(DADMAC) and $AuCl_4^{2-}$ ions decrease the mobility of the later, lengthening their lifetime and making more probable the oxidation of coordinated CH_3OH molecules by the metal centers.

Partial stabilization of Au(II) by linear poly(DADMAC) together with a high $[CH_3OH]$ also accounts for the chain photoreduction of $AuCl_4^-$ in methanol solutions of the polymer. $AuCl_4^{2-}$ disproportionates rapidly in the absence of the polymer and exists only as a short-lived transient unable to react with CH_3OH, which explains the lack of chain reactions under these conditions.[13,22] Au(II) is known to react with O_2 and H_2O_2;[32] the fact that consumption of $AuCl_4^-$ is negligible during most of the induction period is an indication that the oxygen attack regenerates the Au(III) complex. In contrast, the oxidative attack of peroxide induces no net loss of Au(II) ions because this reaction is anticipated to yield $\cdot OH$ in a way analogous to step 5, and this radical induces reformation of $AuCl_4^{2-}$ through steps 6 and 3.

Conventional chain photoreactions usually comprise second-order terminations of the chain carriers, and have rate laws that are linear functions of the square root of I_0.[35] In contrast, the linear dependence of $r(-AuCl_4^-)$ on I_0 portrayed in Figure 6 is evidence that termination is a first-order process. Addition of $\cdot CH_2OH$ to one of the double bond of unpolymerized DADMAC is not a viable first-order termination in CH_3OH. As shown earlier,[36] addition of alcohol radicals to the monomer yields an intermediate that undergoes cyclization, but the resulting cyclic radical abstracts a H atom from the solvent, regenerating another alcohol radical. Steps 5−8 were found to be important reactions during the chain reduction of H_2O_2 in methanol,[28] and are useful to explain the atypical independence of $PE(-AuCl_4^-)$ on light intensity presented in the inset of Figure 6. These results imply that the efficiency of the photoreduction is not controlled by the concentration of chain carriers and are understood in terms of a competition between steps 5 and 7.

H_2O_2 formed via reaction 1 accumulates in the gels until most O_2 is consumed, at which moment photobleaching of $AuCl_4^-$ starts. Steps 5 and 7 follow pseudofirst-order rate laws at this point because [peroxide] $\gg$ $[\cdot CH_2OH]$, but the former is not a termination reaction since step 6 regenerates $\cdot CH_2OH$ radicals, $k_6 = 9.7 \times 10^8$ M^{-1} s^{-1}.[28] Step 7 initiates termination, and the fraction of radicals involved in this reaction is $f_7 = r_7/(r_5 + r_7)$, where r_5 and r_7 are the rates of steps 5 and 7, respectively. Simplification yields $f_7 = k_7/(k_5 + k_7)$, or $f_7 = 4.5 \times 10^{-2}$ using $k_5 = 6 \times 10^4$ M^{-1} s^{-1} and $k_7 = 2.8 \times 10^3$ M^{-1} s^{-1}.[28] This means that of the radicals reacting with the peroxide, the percent lost via reactions 7 and 8 remains constant at 9% irrespective of $[\cdot CH_2OH]$ and $[H_2O_2]$. Therefore, the fraction of radicals involved in propagations is the same for all I_0 values, leading to the unusual dependencies of Figure 6. Participation of H_2O_2 in the $AuCl_4^-$ photoreduction for gels initially containing air is also useful to rationalize the slower reactions of N_2-saturated systems. In the latter case, no H_2O_2 is formed and $\cdot CH_2OH$ radicals that fail to react with $AuCl_4^-$ decay via disproportion-

ations and dimerizations ($2k_9 = 1.6 \times 10^9$ M^{-1} s^{-1})[28]

$$2{\cdot}CH_2OH \rightarrow \text{products} \qquad (9)$$

termination step 9 leads to the irreversible loss of these radicals and to shorter chains.

During most of the photobleaching [$AuCl_4^-$] remains very high, implying that the majority of the photons entering the gel are absorbed by this complex. Thus, the initiation rate (r_2) is expected to be time-invariant and to follow the rate law $r_2 = I_0\phi_i$, where ϕ_i is the initial reduction quantum yield of $AuCl_4^-$, ($\phi_i = 0.1$).[13] Propagation step 3 is the main path for the consumption of Au(III), meaning that PE($-AuCl_4^-$) $= r_3/I_0$, where r_3 is the rate of this reaction. The kinetic chain length (kcl) is equal to $r_3/r_2 = PE(-AuCl_4^-)/\phi_i$; kcl values between 84 and 306 are obtained from the data of the inset in Figure 4. The occurrence of such long chains allows derivation of a rate law for the photoreduction using standard steady-state approximations.[35] These assumptions are that initiation is the rate-determining step, that the rates of initiation and termination are equal ($r_2 = r_7$), and that all propagation rates are equal ($r_3 = r_4$) and much higher than the termination rate. The first assumption of a rate-determining initiation is consistent with the lack of rate changes upon substitution of CH_3OH by CD_3OD. Since $AuCl_4^-$ is reduced mainly via step 3

$$r(-AuCl_4^-) = k_3[AuCl_4^-][{\cdot}CH_2OH] \qquad (10)$$

Using $r_2 = r_7$ yields [$\cdot CH_2OH$] $= I_0\phi_i/k_7'$, where $k_7' = k_7[H_2O_2]$, and [$\cdot CH_2OH$] is the steady-state concentration of the chain carriers. After substitution the reduction rate is

$$r(-AuCl_4^-) = (I_0\phi_i k_3/k_7')[AuCl_4^-] \qquad (11)$$

Equation 11 predicts a linear variation of $r(-AuCl_4^-)$, or of PE($-AuCl_4^-$), with [$AuCl_4^-$] and the data presented in the inset of Figure 4 indicates that the photonic efficiency follows such relationship at Au(III) concentrations between 5 and 9.5 mM. Using the slope ($\phi_i k_3/k_7' = 1.7 \times 10^3$ M^{-1}) results in $k_3/k_7' = 2.8 \times 10^4$ M^{-1}. Furthermore, as predicted by eq 11, a straight line is obtained by plotting r($-AuCl_4^-$) vs I_0 (Figure 6), whereby the slope ($26.4 = (\phi_i\, k_3/k_7')[AuCl_4^-]$) yields $k_3/k_7' = 4.4 \times 10^4$ M^{-1}. Although evaluation of k_3 is not possible in the absence of an experimental value for [H_2O_2], the good agreement of the k_3/k_7' values derived from the two different sets of data provide further support for the proposed mechanism. The resulting self-consistent kinetic parameters suggest that similar peroxide concentrations are present in all gels when the $AuCl_4^-$ reduction starts.

The mechanistic analysis based on the premise that, excluding reaction 4, all other steps proceed as in homogeneous solution is unable to account for matrix-induced kinetic effects. For instance, the data of Figure 4 are described well by eq 11 at [$AuCl_4^-$] $< 1 \times 10^{-2}$ M, but divergence from the predicted behavior is evident at this concentration and above. The deviations are related, in part, to decreases in the gel volume that occur when [$AuCl_4^-$] is higher than 10 mM. Deswelling of polyelectrolyte gels is influenced by high electrolyte concentrations and solvents less polar than water.[37] Attempts to evaluate quantitatively the effect of electrolytes on the swelling behavior of highly charged gels have shown that the mobility of counterions as well as their association with the matrix play an important role.[38] Ion-pairing not only decreases the osmotic pressure of the counterions, but the ion pairs can aggregate via dipole−dipole attractions to form microdomains. Partial exclusion of CH_3OH from these regions yield ionic cross-links that accentuate deswelling. Binding of Cl^- to ammonium cations of the poly(DADMAC) gel represses swelling in water, and contractions similar to those induced by $AuCl_4^-$ take place when the gels are exposed to comparable concentrations of chloride (> 10 mM).[37a] These findings provide evidence that $AuCl_4^-$ interacts with these gels in a way analogous to Cl^-.

Formation of ion pairs and microdomains must be substantial at the high [chloride] present in the swollen polymer, particularly in the less polar CH_3OH. These processes are enhanced by anions more polarizable than Cl^-, such as $AuCl_4^-$, and are believed to increase exponentially when the gel composition approaches the value of macroscopic deswelling.[37] Although microdomains are abundant when the [electrolyte] is slightly lower than that at which the gel shrinks, solvent molecules excluded from these regions increase the volume of places with less extensive ion-pairing, and no net deswelling is noticed. This occurs at 10 mM $AuCl_4^-$ for poly(DADMAC) gels, where the sharp maximum of PE($-AuCl_4^-$) shown in Figure 4 coincides with the large increases in ion-paired structures. Therefore, photobleaching is aided by ion pairing; the high [$AuCl_4^-$] in microdomains favors initiation, whereas the lower mobility of the formed Au(II) ions favors step 4. At [$AuCl_4^-$] > 10 mM the gels shrink, imposing spatial limitations to the diffusion of chain carriers. Further examples of the restricting effect induced by the matrix are the slower photoreactions with gels prepared using less swelling solution (PM/SV $= 5.04 \times 10^{-2}$ g mL^{-1}), or with heavily γ-irradiated polymers that have higher than normal cross-link densities.

As a result of the high [$AuCl_4^-$] most of the photons entering the gels are initially absorbed within a narrow region close to the tube wall, which explains the inward Au(III) bleaching that starts at the polymer-glass interface. However, the sequential consumption of $AuCl_4^-$ from bottom to top suggests that the chain reaction propagates preferentially along planes perpendicular to the vertical axis of the gel. Such peculiar sequence of events is a reflection of the [O_2] gradient established under illumination, where this concentration increases with decreasing distance to the air-filled headspace above the polymer. $AuCl_4^-$ reduction is efficient in regions with a low [O_2]; this concentration remains small despite the continuous flow of air down the gel because part of the radicals formed in steps 2 and 4 react with the gas. Bleaching of Au(III) is less efficient when $\cdot CH_2OH$ radicals diffuse upward since the oxygen-inhibiting effect is accentuated by the increasing [O_2] in this direction. This rationalization is supported by the occurrence of a second induction period when photolysis is interrupted long enough to allow replenishment of oxygen, and by the sequence reversal that takes place during the reformation of $AuCl_4^-$ induced by O_2.[18]

The proposed mechanism predicts $AuCl_2^-$ as the main product, but the amount present at the end of the induction period represents less than 20% of the reduced $AuCl_4^-$. Formation of Au(I) species other than $AuCl_2^-$ is unlikely considering the high [Cl^-] in the gels and the large formation constant of the complex ($\beta_2 > 10^9$).[29] Reduction of $AuCl_2^-$ by $\cdot CH_2OH$ is thermodynamically feasible because $E°$ (CH_2O, H^+/$\cdot CH_2OH$) $= -1.18$ V,[39] and $E° \approx 0.6$ V was estimated for ($AuCl_2^-/AuCl_2^{2-}$) in aqueous 2-propanol.[22] This reduction is only a side reaction that consumes chain carriers because mechanisms including such step are unable to account for the different rates of gels with and without air. Previous results showed that photogeneration of Au in polymer-free CH_3OH solutions occurs after the bleaching step is completed and proceeds faster when [$AuCl_4^-$] increases.[18] These observations

seem to support a disproportionation of $AuCl_2^-$ to produce metal

$$3AuCl_2^- \leftrightarrow 2Au + AuCl_4^- + 2Cl^- \qquad (12)$$

Although the equilibrium is displaced to the right side in aqueous HCl solutions ($K = 1 \times 10^8$), the forward reaction is very slow even on the surface of metallic gold.[40] Accumulation of reduction products followed by their transformation to Au particles after irradiation also occurs when $AuCl_4^-$ is reduced radiolytically.[22] These findings were attributed to a rather gradual disproportionation of Au(I) on the surface of metal crystallites.

Although two consecutive transformations also take place in the gels, regeneration of $AuCl_4^-$ is the only process noticed if photolysis stops at the end of the induction period, without simultaneous production of metal. Particles form exclusively under illumination, meaning that the formation process is not a direct consequence of reaction 12. Instead, an absorption centered at 360 nm is observed during the last stage of the photobleaching step in Figure 1, which is not detected in the absence of gels,[18] or in radiolysis experiments.[22] Considering that $AuCl_4^{2-}$ and $AuCl_4^-$ exhibit nearly identical spectra,[35] and that Au(II) is air-sensitive,[34] it is clear that the former ion is not responsible for the (air-stable) signal at 360 nm. Reduction of $AuCl_4^-$ by poly(ethyleneglycol) generates a transient with a similar absorption ($\lambda_{max} = 380$ nm), that is a direct precursor of Au particles.[25] Analogous signals are displayed by cationic polynuclear complexes (known as Au clusters) consisting of gold atoms and Au(I) ions bound by phosphine ligands.[41] The data of the thermal, radiolytic and photochemical studies are mutually consistent if the Au atoms formed via a reaction similar to 12 combine with $AuCl_2^-$ yielding gold clusters containing metal atoms bound to Au(I) ions. Although the clusters transform to metal crystallites in the absence of stabilizers, they are partially stabilized by poly(ethyleneglycol) or poly(vinyl alcohol).[22,25]

Following this interpretation, the species responsible for the signal centered at 360 nm is assumed to be an Au cluster, denoted Au_c. Only relatively hard ligands are present in the gels but evidence exists that stable gold clusters are generated in them. For example, Au_c is not affected by O_2 or H_2O_2 since the signal at 360 nm is not altered when photolysis is stopped for a time long enough to increase $[O_2]$, causing another induction period. The constant strength of this signal irrespective of $[AuCl_4^-]$, I_0 and the PM/SV value implies that $[Au_c]$ is invariant in all gels independent of the concentrations of $AuCl_2^-$, ion pairs and microdomains. Such behavior suggests that saturated solutions of Au_c exist within cavities of the gel, with the solutions being at equilibrium with nonabsorbing polynuclear gold complexes electrostatically bound to the matrix. This explanation is consistent with the lack of changes in the 360 nm absorption during particle generation because any consumed Au_c is reformed at the expense of the bound clusters. Considering that Au_c is the main absorber of the 350 nm radiation at the end of the induction period, it seems logical to assume that metal formation is initiated by the cluster, and to relate the apparent zero-order kinetics of this process (Figure 2) to the constant $[Au_c]$ that exists throughout the photoreaction.

The role of Au_c on the formation of particles is better understood after examining several kinetic features shared by this process and the photobleaching step. The progress of both photoreactions is hindered by the presence of a high $[O_2]$ but they proceed faster for gels prepared under air. Also, their rates decrease when the gels shrink and upon diluting CH_3OH with H_2O. Both photoreactions are confined to the same gel regions, follow a similar sequence of events and exhibit large PE values typical of chain reactions. These findings are evidence that $\cdot CH_2OH$ radicals and H_2O_2 participate as well in the crystallite generation. While the lack of compositional information about Au_c precludes formulation of a detailed mechanism for this process, the post-irradiation reaction (Figure 2) suggests that chain carriers are produced when particles form. A plausible sequence of events involves a photoreduction step of Au_c analogous to 2, followed by collision and fusion of the reduced cluster with matrix-bound clusters. Disproportionation of Au(I) ions from the colliding clusters produces Au(II), which generates $\cdot CH_2OH$ radicals via step 3. Interestingly, the simplest mechanism that yields an apparent zero-order rate law for particle generation proportional to I_0^2 is based on a biphotonic (rate-determining) initiation, chain propagations through cluster−cluster reactions that eventually form Au particles, and termination via step 7. No such agreement is obtained from mechanisms that involve a monophotonic initiation and particle formation steps via cluster−cluster dimerizations.

According to the data of Figure 7, particles are generated via an unusual biphotonic chain reaction that has not been observed in homogeneous systems.[13,22] This process is unexpectedly efficient because according to the cluster spectrum, only 37% of the 350 nm photons can be absorbed by Au_c at the end of the induction period. Obviously, the chances of a consecutive two-photon absorption by Au_c are even lower, and decrease further when the light-absorbing Au crystallites form. However, according to the data of Figure 2 the rate of particle generation remains unchanged with time, which can be rationalized after considering that particles form sequentially as layers. Although these structures are easier to detect in gels made with a lower [monomer],[18] crystallite ordering is evident in all cases. The plasmon signal of spherical Au particles intensifies without large changes above 650 nm when colloidal gold is generated.[22,24,25] In contrast, apart from the strengthening of the plasmon signals, o.d. increases throughout the range of wavelengths when particles form in the gels (Figure 1), which resembles closely the optical changes accompanying the stacking of nanometer-thick layers of Au crystallites.[42]

Generation of a layer starts in a region initially free of particles and proceeds horizontally toward the interior of the gel. Preexisting Au crystallites located underneath the region where a new layer is produced are unable to interfere with the photoreaction. Particle formation within the new layer continues until they reach a concentration high enough to out-compete Au_c for the photons. At this point, the rate of the formation process decreases and, simultaneously, crystallites start being photogenerated in the next layer. Hence, continuous generation of Au crystallites initiated by Au_c is possible due to the anisotropic particle distribution in the gel and the self-limiting nature of the photoreaction.

Differences in the behavior of the photobleaching of $AuCl_4^-$ and of the particle photogeneration process become evident when cycles of illuminations and dark periods are performed at regular time intervals. Only slight increases in the rates of photobleaching are noticed in Figure 8, when the dark period between consecutive cycles of particle formation and decay is long enough to allow an almost complete reformation of $AuCl_4^-$. The shorter induction periods of gels photolyzed after only 3 days without light are a trivial outcome of incomplete reformation of $AuCl_4^-$ during this time. In contrast, PE(Au_n) improves vastly with increasing number of cycles even for dark intervals of 2 weeks. Particle formation induces changes that fade away only after storing the gels for several months, suggesting that

these are reversible structural alterations, which in poly(DADMAC) gels are known to occur very slowly.[37] Experiments with square curvettes clearly show that generation of Au crystallites increases the internal pressure of the gels, shattering the cells. Formation of the metallic phase is expected to disrupt ionically cross-linked microdomains. Subsequent oxidation of the crystallites results in less ordered microdomains, facilitating generation of metal during the next cycle. This "memory effect" is further evidence that the interesting processes taking place in the photoadaptive gels result from effects due to the chemical properties of Au in conjunction with properties of the polymer matrix.

Acknowledgment. We thank L. Iton for useful discusssions, P. Mitchell and M. E. Miller for helping us with XRD and TEM measurements, R. Knight for his help during gamma irradiations and D. Stanbury for making the HP 8452 instrument available to us. K. M. and S. W. are grateful to Auburn University for fellowships through the PGOP program. This work was supported by the NSF EPSCoR Program.

References and Notes

(1) McArdle, C. B., Ed. *Applied Photochromic Polymer Systems*; Blackie & Son: Glasgow, 1992.

(2) Dotsenko, A. V.; Glebov, L. B.; Tsekhomsky, V. A. *Physics and Chemistry of Photochromic Glasses*; CRC Press: Boca Raton, 1998.

(3) Araujo, R. G.; Borrelli, N. F. In *Optical Properties of Glasses*; Uhlmann, R., Kreidl, N. J., Eds.; American Ceramic Society: Westerville, Ohio, 1991; p 125.

(4) Levy, D. *Mol. Cryst. Liq. Cryst.* **1997**, *297*, 31.

(5) Kamat, P. V. *Prog. Inorg. Chem.* **1997**, *44*, 273.

(6) (a) Sahyun, M. R. V.; Hill, S. E.; Serpone, N.; Danesh, R.; Sharma, D. K. *J. Appl. Phys.* **1996**, *79*, 8030. (b) Serpone, N.; Lawless, D.; Sahyun, M. R. V. *Supramolecular Chem.* **1995**, *5*, 15.

(7) (a) Sahyun, M. R. V.; Serpone, N.; Sharma, D. K. *J. Imaging Sci.* **1993**, *37*, 261. (b) Micic, O. I.; Meglic, M.; Lawless, D.; Sharma, D. K.; Serpone, N. *Langmuir* **1990**, *6*, 487.

(8) Pal, T.; Sau, T. K.; Jana, N. R. *Langmuir* **1997**, *13*, 1481.

(9) Belloni, J. *Radiat. Res.* **1998**, *150* (Suppl.), S9.

(10) Li, W.; Virtanen, J. A.; Penner, R. M. *Langmuir* **1995**, *11*, 4361.

(11) Kreibig, U.; Vollmer, M. *Optical Properties of Metal Clusters*; Springer-Verlag: Berlin, 1995.

(12) Irie, M.; Ikeda, T. In *Functional Monomers and Polymers*; Takemoto, K.; Ottenbrite, R. M.; Kamachi, M. Eds.; Marcel Dekker: New York, 1997; p 65.

(13) (a) Kartuzhanskii, A. L.; Studzhinskii, O. P.; Plachenov, B. T.; Sokolova, I. V. *J. Appl. Chem. USSR* **1986**, *59*, 2265. (b) Studzhinskii, O. P.; Kartuzhanskii, A. L.; Plachenov, B. T. *J. Appl. Chem. USSR* **1985**, *55*, 597.

(14) (a) Alvarez, M. M.; Khoury, T.; Schaaff, T. G.; Shafigullin, M. N.; Vezmar, I.; Whetten, R. L. *J. Phys. Chem.* B **1997**, *101*, 3706. (b) Lamber, R.; Wetjen, S.; Schulz-Ekloff, G.; Baalmann, A. *J. Phys. Chem.* **1995**, *99*, 13834. (c) Duff, D. G.; Baiker, A.; Edwards, P. P. *Langmuir* **1993**, *9*, 2301.

(15) Cadle, S. H.; Bruckenstein, S. *J. Electroanal. Chem.* **1973**, *48*, 325.

(16) Enüstün, B. V.; Turkevic, J. *J. Am. Chem. Soc.* **1963**, *85*, 3371.

(17) Meldrum, F. C.; Heywood, B. R.; Mann, S. *J. Colloid Interface Sci.* **1993**, *161*, 66.

(18) Weaver, S.; Taylor, D.; Gale, W.; Mills, G. *Langmuir* **1996**, *12*, 4618.

(19) Huber, E. W.; Heineman, W. R. *J. Polym. Sci., Polym. Lett.* **1988**, *26*, 333.

(20) Suzuki, A.; Tanaka, T. *Nature* **1990**, *346*, 345.

(21) Heller, H. G.; Langan, J. R. *J. Chem. Soc., Perkin Trans. 2* **1981**, 341.

(22) Gachard, E.; Remita, H.; Khatouri, J.; Keita, B.; Nadjo, L.; Belloni, J. *New J. Chem.* **1998**, 1257.

(23) Kunkely, H.; Vogler, A. *Inorg. Chem.* **1992**, *31*, 4539.

(24) Quinn, M.; Mills, G. *J. Phys. Chem.* **1994**, *98*, 9840.

(25) (a) Longenberger, L.; Mills, G. *Nanotechnology: Molecularly Designed Materials*; Chow, G.-M., Gonsalves, K. E., Eds; ACS Symposium Series 622, American Chemical Society: Washington D. C., 1996; p 128. (b) Longenberger, L.; Mills, G. *J. Phys. Chem.* **1995**, *99*, 475.

(26) (a) Battino, R.; Rettich, T. R.; Tominaga, T. *J. Phys. Chem. Ref. Data* **1984**, *13*, 563. (b) Stephen, H.; Stephen, T. *Solubilities of Inorganic and Organic Compounds*; Pergamon Press: Oxford, 1963; Vol. 1, part 1, p 570.

(27) Alfassi, Z. *Peroxyl Radicals*; John Wiley: Chichester, 1997.

(28) Ulanski, P.; von Sonntag, C. *J. Chem. Soc., Perkin Trans. 2* **1999**, 165.

(29) Keim, R., Ed.; *Gmelin Handbook of Inorganic and Organometallic Chemistry, Gold*, 8th ed.; Springer-Verlag: Berlin, 1992, Supplement Vol. B1, pp 180−258.

(30) Weiser, H. B. *Inorganic Colloid Chemistry*; John Wiley: New York, 1933; Vol I, p 35.

(31) Bornstein, L.; Chernysov, D.; Valetsky, P.; Tkachenko, N.; Lemmetyinen, H.; Hartmann, J.; Forster, S. *Langmuir* **1999**, *15*, 83.

(32) Rich, R. L.; Taube, H. *J. Phys. Chem.* **1954**, *58*, 6.

(33) Gosh-Mazumdar, S.; Hart, E. J. *Adv. Chem. Ser.* **1968**, *81*, 194.

(34) De Castro, E. S.; Huber, E. W.; Villarroel, D.; Galiatsatos, C.; Mark, J. E.; Heineman, W. R. *Anal. Chem.* **1988**, *59*, 134.

(35) Huyser, E. S. *Free-Radical Chain Reactions*; Wiley-Interscience: New York, 1970; Chapter 3.

(36) Naim, A.; Mills, G.; Shevlin, P. B. *Tetrahedron Lett.* **1992**, *33*, 6779.

(37) (a) Starodoubtsev, S. G.; Khokhlov, A. R.; Sokolov, E. L.; Chu, B. *Macromolecules* **1995**, *28*, 3930. (b) Philippova, O. E.; Pieper, T. G.; Sitnikova, N. L.; Starodoubtsev, S. G.; Khokhlov, A. R.; Kilian, H. G. *Macromolecules* **1995**, *28*, 3925.

(38) Siegel, R. A. In *Advances in Polymer Science*, Dusek, K., Ed.; Springer-Verlag: Berlin, 1993, vol. 109, p 233.

(39) Schwarz, H. A.; Dobson, R. W. *J. Phys. Chem.* **1989**, *93*, 409.

(40) Lingane, J. J. *J. Electroanal. Chem.* **1962**, *4*, 332.

(41) Hall, K. P.; Mingos, D. M. In *Progress in Inorganic Chemistry*; Lippard, S. J., Ed.; John Wiley: New York, 1984; vol. 32, p 237.

(42) Musick, M. D.; Peña, D. J.; Botsko, S. L.; McEvoy, T. M.; Richardson, J. N.; Natan, M. J. *Langmuir* **1999**, *15*, 844.